Small to mid-sized stellarator experiments: topology confinement and turbulence

J. H. Harris

Plasma Research Laboratory
Research School of Physical Sciences and Engineering
The Australian National University
Canberra ACT 0200
Australia

Abstract. *The very large stellarator experiments LHD (operating) and W7X (under construction) move stellarator-confined plasmas into the near-reactor regime. Continuing experiments on smaller devices operating at heating powers from kW to a few MW are exploring the effects of magnetic configuration stability and turbulence on plasma confinement to improve stellarator performance and our understanding of general toroidal confinement physics. Key issues being explored are the relation of rational magnetic surfaces and magnetic configuration characteristics such as helical ripple to plasma transport, confinement scaling and turbulence. The robust macroscopic stability of currentless stellarator plasma is a major contributing factor to theses studies. Many of the phenomena most clearly evident in stellarators are increasingly implicated in tokamak experiments as well.*

PACS: 52.55.Hc 52.35.Dy 52.55.Tn 52.35.Ra

1. Introduction

Stellarator devices—which comprise all the toroidal plasma confinement configurations (e.g. "advanced" stellarators, heliotrons, torsatrons, heliacs, etc) which produce magnetic surfaces with rotational transform—share many of the confinement properties of tokamaks, without the need to drive and maintain plasma current. The largest stellarator devices, the presently operating LHD (Motojima et al 2003, Motojima et al, 2004) and W7X (under construction, Fest et al, 2004) are advancing stellarator physics to the near-reactor regime. However, existing small-to-medium stellarators, with plasma minor radii < 20 cm, magnetic fields ranging from 0.1 T to 2 T, and heating powers ranging from a few kW to a few MW, are providing considerable information and guidance for the development of the stellarator concept. The stellarator's key feature—its lack of plasma current—allows experiments on smaller devices to explore phenomena that scale to large devices operating at much higher density, temperature and power with out the complicating factors of current-driven instabilities and runaway electrons.

2. Magnetic configurations of stellarator devices

The principle features distinguishing various members of the stellarator family are the toroidal aspect ratio, the rotational transform profile, and the details of the helical ripple that forms the helical field.

Low-shear, moderate transform stellarators in the present generation of experiments include WEGA (R = 0.7 m, R/a ~ 4) (Otte et al, 2003), TJ-K (R = 0.6 m)(Lechte et al, 2004), and W7AS (R = 2 m, R/a ~ 10) (Geiger et al, 2004). These devices have

radically different coil sets: WEGA is a "classical" stellarator with multipolar-helical windings and separate toroidal field (TF) coils. TJ-K is a torsatron with a single $l = 1$ unidirectional helical winding, and W7-AS is an "advanced" modular-coil stellarator. Typically, these devices have rotational transforms of 0.2-0.7.

Low-shear, high-transform stellarators get much of their rotational transform from the torsion of a spatially-twisting magnetic axis (as envisioned in the original figure-8 scheme of Spitzer). The heliac devices—TJ-II (R = 1.5 m, R/a ~ 7) (Alejaldre et al 2001) and H-1NF (R = 1 m, R/a = 5) (Hamberger et al, 1990) use TF coils helically displaced around a combination circular and helical winding to produce transforms variable from ~0.7 to ~2, much the widest transform variation available in any stellarator. The HSX experiment (R ~ 1.2 m, R/a = 10) (Likin et al, 2003) uses modular coils to achieve near-helical symmetry. The W7X device (under construction), with a transform profile near 1 (above or below), also falls into this general category: it uses helically displaced modular coils to form a "helias" configuration (Beidler et al, 2001, Kleiber et al 2003) which is optimised for MHD properties and orbit confinement.

Moderate-shear, moderate transform stellarators such as CHS (R ~1 m, R/a = 5) (Okamura et al, 1999) and LHD now all use the $l = 2$ heliotron-torsatron architecture, in which two unidirectional helical windings provide both the helical and toroidal field. These configurations achieve their greatest degree of flexibility using a variable external vertical field (VF) to move the flux surfaces inward and outward in major radius, which allows their particle confinement and MHD properties to be optimised/anti-optimised in a variable fashion.

These existing devices operate at aspect ratios of 5-10. A new class of low aspect ratio stellarators ($R/a \leq 4$) is now being developed using both quasi-axisymmetry (QAS) and quasi-poloidal symmetries (QPS) to optimise orbit confinement. At these low aspect ratios, it is necessary to add modest plasma currents to supplement the rotational transform provided by the modular coils. These schemes will be tested experimentally in the NCSX (Reiman et al, 1999) and QPS (Spong et al, 2004) experiments now under construction.

3. Resonant magnetic surfaces

Magnetic surfaces having rational values of rotational transform $\iota = n/m$ play a special role in all toroidal confinement systems, but their role is especially clear in experiments on low-shear stellarators. Figure 1 shows a rotational transform scan carried out in the W7-AS experiment (Brakel et al, 1997) by varying the modular and TF coils currents so as to scan the edge rotational transform through the range $0.2 < \iota < 0.7$. Characteristic maxima and minima can clearly be seen, with the largest maxima falling just above and below low-order rational resonances. These gaps coincide with regions of low rational number density along the number line. Knowledge of the magnetic field structure from e-beam mapping suggests that the observed minima in confinement are not simply due to reduction of the plasma radius by magnetic islands.

Such features are seen both at $\iota < 1$ in "traditional" stellarators (Carreras et al, 1988) and in heliacs at $\iota > 1$ (Herranz et al, 2000; Alejaldre et al, 2001; Harris et al, 2004). Fine-scale Thomson scattering studies of profiles in the RTP tokamak (Lopes-Cardozo et al, 1997) show similar phenomena.

While it is not yet clear just what produces the enhanced transport at resonances, one obvious possibility for a loss mechanism is some sort of fluctuation or turbulence. Low power stellarator experiments offer a means to examine this in plasmas at very low pressure, where finite-β effects are not important.

Experiments on the HSX stellarator suggest that Alfvenic instabilities may be at work here.. Figure 2 shows the results of an HSX experiment using electron-cyclotron heating (ECH) in which low-frequency globally coherent density and magnetic fluctuations were observed at $\iota \sim 1.07$ in configurations with quasi-helical symmetry. The fluctuations disappeared when the symmetry was spoiled using a small (10%) auxiliary TF ripple field. Measurements of X-ray emission suggest that fast (keV) electrons are well-confined in the quasi-symmetric configuration, but poorly confined in the non-symmetric configuration. The coincidence suggests that the fast electrons produced by ECH act to destabilise the plasma. Variation of the density and the working gas in HSX show that the observed fluctuation frequency varies with the Alfven speed $v_A = (B^2/2\mu_0\rho)^{1/2}$, where ρ is the mass density.

These results suggest that a mechanism like the global Alfven eigenmode (GAE) might be operating even in these very low power stellarator discharges. Such fluctuations have been identified in megawatt neutral beam injection experiments in W7AS (Geiger et al, 2004) where injected fast ions resonate with Alfven waves. For these instabilities, the observed frequency is lowered from the Alfven frequency by the small parallel wave number near resonant values of ι:

$$\omega_{GAE} \leq k_{//} v_A = (m\iota - n) v_A / R \qquad (2)$$

but the instability disappears on the resonance itself.

Data from H-1NF add support for this picture. Figure 3(a) shows how the magnetic fluctuation frequency tracks the square-root of the density in low density discharges. In other discharges (Fig. 3(b)), frequency jumps coincide with decrements in density, suggesting that the active resonance changes location on the rotational transform profile. In these discharges, the fast particles would also have to be electrons to match the Alfven speed. Hard-X ray emission is indeed seen during ICRF, and is being studied further to firm up the connection.

It thus appears that specific magnetic fluctuations at least signal the change of pressure gradients near rational surfaces, and are perhaps related to the local flattening of the gradient that is expected theoretically (Boozer, 1984; Boozer, 2004).

Similar phenomena are seen in reversed shear tokamak discharges. In the DIIID tokamak (Jayakumar, 2004; Austin, 2004). As q passes through rational values, local increases are seen in the electron temperature. Similar improvements in local confinement are also seen in JET reversed-shear discharges, and the formation of these internal transport barriers is signalled by cascades of Alfven activity as q passes through high order rational values towards a gap near a major resonance (Joffrin et al, 2002).

The mechanism for the formation of the transport barrier (ITB) near resonances itself

remains unclear; observations in CHS of discontinuities in the electric potential near rational surfaces suggest that these locations favour the development of E x B shear and subsequent ITB formation (Fujisawa, 2004).

4. Edge magnetic islands and confinement improvement

During stellarator design and construction, strenuous efforts are made (see for example, Carreras et al, 1988; Hamberger et al, 1990; Feist et al, 2004) to eliminate resonant magnetic field components with normalised amplitudes > a few parts in 10^4 so as to avoid producing large magnetic islands in the vacuum field of the confinement volume that reduce the effective confinement volume.

Typically, small naturally occurring islands (inherent in the coil structure) determine the last closed flux surface. Careful manipulation of these edge islands by varying the rotational transform or deliberately exciting additional perturbation fields can actually provoke transitions to high confinement regimes.

This effect was first seen in W7-AS discharges with $\iota = 0.5$, in which L-H transitions were observed provided that the plasma was limited magnetically rather than by a material limiter (Erckmann et al, 1993). Recent experiments in Heliotron-J (Sano et al, 2004) have explored similar phenomena in detail, and have found preferred windows at edge $\iota = 0.55$ and 0.625. The differences between configurations that exhibit L-H transitions and those that do not are subtle indeed, and the authors find they cannot be simply explained by theories based on poloidal viscosity and the magnetic structure. This suggests that three-dimensional electric field structures and the connection of the plasma to the wall play a crucial role.

The alteration of the radial electric field due to island formation has been explicitly demonstrated by experiments on the TJ-II heliac (Hidalgo et al, 2002; Pedrosa et al, 2004), whose results are summarised in Fig. 4. Measurements with Mach probes and a heavy ion beam probe (Melnikov et al, 2004) show, respectively the development of velocity and radial electric field shear in the region near the island. The measurement of these effects using completely independent diagnostic techniques makes these observations persuasive.

Spectroscopic and "cold-pulse" pellet studies in the large LHD experiment (Ida et al, 2004) have demonstrated that a deliberated induced island at $\iota = 1$ produces electric field shear and a reduction of heat transport in the vicinity of the island. A theoretical model (Shaing, 2002) for understanding these phenomena treats the island as a self-contained non-axisymmetric confinement region wherein the requirement for ambipolar transport drives the generation of radial electric fields.

Detailed fundamental studies of the role of magnetic islands in altering local confinement properties can usefully be done on a controlled small scale experiment at low power, in which probes can be used to measure plasma parameters, flows, etc. on a very small scale. Such work is now being started on the revitalised WEGA stellarator (now at IPP-Greifswald) operating at low magnetic fields of 87.5 mT (Otte et al, 2003). A special challenge for these low field experiments is developing a sufficiently central heating technique so as to facilitate measurements of the effect of the islands on local confinement.

Experiments on the W7-AS stellarator (McCormick et al, 2002) and the DIII-D tokamak (Evans et al, 2004) show that judiciously induced island chains near the plasma edge result in high-confinement discharges with desirable characteristics such as the suppression of edge-localised modes (ELMs) and the redistribution of particle and heat flux. These results suggest that magnetic islands can be a powerful tool for seeding beneficial changes in plasma confinement properties in both stellarators and tokamaks.

5. Cross-configuration study of confinement scaling

As in the case of tokamaks, scaling studies of the parameter dependence of global energy confinement in stellarator devices have proved useful in planning experiments, measuring progress, and focusing research on the key physics issues affecting confinement performance. The first such study for stellarator confinement was the International Stellarator Scaling (ISS) study (Stroth et al, 1995) which established a basic scaling similar to that used in tokamak research. A follow up scaling study to extend this effort to encompass more recent stellarator results and new experiments began in 2003, and has assembled a database of ~2500 entries from experiments on W7A, W7-AS, Heliotron-E, Heliotron-J, CHS, LHD, ATF, and TJ-II (Yamada et al, 2004a). . Statistical analysis of these data (Yamada et al, 2004b) shows that a common scaling relation can be used to describe the dependence of confinement times on the usual parameters of major and minor radii, magnetic field, plasma density, rotational transform, and heating power, provided that a configuration dependent renormalization factor f_{enh} is introduced. The provisional ISS04 relation is given by:

$$\frac{\tau_E^{ISS04v3}}{f_{enh}} = 0.148 a^{2.33} R^{0.64} P^{-0.61} \bar{n}_e^{0.55} B^{0.85} \iota_{2/3}^{0.41} \propto \tau_{Bohm} \rho^{*-0.90} \beta^{-0.14} \nu_b^{*-0.01} \qquad (3)$$

and the relationship with the data is shown in Fig. 5. The exponents in the scaling are similar to those of ISS95, but use a much wider range of data, and now include configuration renormalisation. The details of this relation are still under study, as there is evidence of some co-dependencies in the data sets. A notable feature of the new scaling results is the extension of the range of rotational transforms included in the dataset to $\iota \sim 2$ by virtue of inclusion of data from the TJ-II heliac.

The ISS04 relation is the first to introduce a stellarator configuration-dependent parameter other than the rotational transform (which is also present in tokamak scalings, of course). An attractive candidate as a driver for these differences is the helically-corrugated stellarator magnetic field, whose detailed geometry varies considerably from configuration to configuration even for cases of comparable rotational transform.

Experimental comparisons between different configurations operating at extremes in configuration parameters are viable in stellarators because of their robust MHD equilibrium and stability characteristics. Experiments on W7-AS (Geiger et al, 2004): show that as the plasma pressure increases, the flux surfaces show the expected outward Shafranov shift, and magnetic fluctuations grow and then subside as the volume-average β approaches 3%. This self-stabilisation results from changes to rotational transform that move the various resonances relative to the pressure gradients, an increase in shear, and deepening of the magnetic well due to the outward

shift of the flux surfaces, which is reflected in calculations of Mercier instability. Indeed, it is even possible to shift the plasma inward in radius to begin with, thus starting the pressure increase from a configuration that is Mercier unstable.

These trends hold not only for the low-shear W7-AS configuration, but also the whole range of sheared heliotron/torsatron experiments—CHS (Okamura et al, 1995; Okamura et al, 1999), LHD (Sakakibara et al, 2002; Watanabe et al, 2004; Sakakibara et al, 2004) and ATF (Harris et al, 1989). An additional feature of the sheared configurations is that the observed high-beta stabilisation of MHD activity in the outer region of the plasma in the region where ι approaches 1 (-1.5 in LHD) involves local flattening of the pressure profile.

In sum, it now appears that purely pressure driven interchange-type instabilities are much less virulent in real stellarator plasmas than are their tearing and kink mode cousins in tokamak plasmas. This may reflect the underlying differences in linear growth mechanisms (Furth et al, 1963) or a favourable tendency toward non-linear stabilisation (Ichiguchi et al, 2004), and certainly warrants deeper investigation.

The ability to produce stable plasmas in heliotron/torsatron configurations even under conditions of theoretical instability leads to considerable freedom to explore the role of the helically rippled stellarator field in plasma confinement by pushing the plasma into regions of lower or higher ripple. This technique was developed in experiments on CHS (Okamura et al, 1999) and then extended to the similar LHD configuration (Yamada et al, 2004a).

The principle is illustrated in Fig. 6. When the flux surfaces in CHS (or LHD) are shifted inward in major radius using an external vertical field, the configuration develops a magnetic hill or anti-well, a situation which ought to be unstable but in practice is not. This inward shift also alters the particle drift orbits by changing the relationship of the magnetic surfaces to the mod-B contours such that trapped particle orbits are better centred. This is illustrated in Fig. 6 using 3.5 MeV trapped-alpha orbits calculated for a reactor scale configuration shifted appropriately (Murakami et al, 2004). Thus, it is possible to realise experiments in the same device in which the helical ripple is systematically varied.

Comparative experiments in CHS (Okamura et al, 1999) and LHD (Yamada et al, 2004a) have consistently shown that confinement improves when the plasma is shifted inward. To allow comparison of all the experimental devices in the study, a consistent measure of the helical ripple, $\varepsilon_{\mathrm{eff}}$, was calculated for all the configurations used. The definition of $\varepsilon_{\mathrm{eff}}$ was developed (Beidler and Hitchon, 1994) as a measure of the $1/\nu$ transport by deeply trapped particles in the collisionless regime, and has since been widely used as a figure of merit for optimising stellarator configurations (Reiman et al, 1999; Beidler et al, 2001; Tribaldos, 2001; Okamura et al, 2001; Nemov et al, 2003; Spong et al, 2004). While $\varepsilon_{\mathrm{eff}}$ is strictly a measure of $1/\nu$ transport, it is also a rough proxy for other physics processes involving ripple-trapped particles: direct orbit losses, geometrical flow viscosity, and trapped particle instabilities.

Figure 7 shows the configuration-dependent renormalization factors f_{enh} as a function of $\varepsilon_{\mathrm{eff}}$ at the 2/3 radius. The factors increase with decreasing $\varepsilon_{\mathrm{eff}}$, suggesting that

confinement is indeed improved by decreasing the ripple. While it is premature to formally introduce this dependence into the scaling relation, a fit to the upper envelope yields a $\varepsilon_{eff}^{-0.4}$ dependence. This augurs well for the eventual performance of optimised stellarator configuration such as HSX, W7X, NCSX, and QPS, which feature values of $\varepsilon_{\rm eff}$ at least an order of magnitude smaller than those of the previous generation of stellarators.

It is not clear yet just which of the ripple related physics mechanisms might be responsible for the improvement in confinement seen with decreasing $\varepsilon_{\rm eff}$. However, recent experimental measurements of E x B plasma flow induced by electrode biasing are suggestive (Fig. 8). When the device is operated in its quasi-helically symmetric mode ($\varepsilon_{\rm eff} = 0.007$), the induced flow velocity is more than twice that achieved in the mirror mode of operation ($\varepsilon_{\rm eff} = 0.06$). This suggests that low ripple should favour the development of the sheared E x B flow that is a key contributor to improved confinement. An attractive feature of this mechanism is that it can improve confinement over a large range in collisionality.

6. Basic turbulence studies

Studies of plasma turbulence are of fundamental importance because of the role of turbulence in enhanced, non-classical transport. Macroscopically stable, low power currentless stellarator plasmas offer an attractive environment for such studies because they permit detailed diagnostics using insertable probes. Indeed, such devices are essentially toroidal Q machines.

Recent experiments on the TJ-K device (Lechte et al, 2004) using 1.8 kW of 2.45 GHz ECH, magnetic fields of 72-96 mT, and hydrogen, helium, and argon as working gases ($n_e \sim 10^{17}$ m^{-3}, $T_e \sim 10$ eV, $T_i < 1$ eV) , have provided an unusually complete characterisation of turbulence by using a full-coverage poloidal array of 64 Langmuir probes to measure fluctuations in density and potential and their correlations. Detailed, wavenumber-resolved measurements of the cross-phase between density and potential fluctuations showed a phase angle near zero for all experimental conditions, in close agreement with DALF3 code predictions for drift-wave turbulence (Scott, 1997). Studies of the poloidal correlation length $L_{\rm corr}$ (~ eddy size) of the turbulence with the drift scale $\rho_s = c_s/\omega_{ci}$, where c_s is the sound speed, show that $L_{\rm corr}$ is proportional to ρ_s ,(Fig. 9) and that the maximum turbulent particle transport occurs at scale lengths ~ $L_{\rm corr}$, rather than scales of the largest fluctuation amplitude.

Basic turbulence studies on the H-1NF heliac have concentrated on behaviour in the H-mode, which can be accessed at exceptionally low heating power (60 kW of helicon wave heating) low temperatures (10-40 eV) at low fields < 0.2T (Shats et al, 1996). Recent experiments with multiple probe arrays demonstrate radial electric field generation and self-regulation of transport in fluctuating high-confinement modes (Shats et al, 2004). In the example shown in Fig. 10, at t = 50-52 ms, low-frequency (1 kHz) fluctuations in the radial electric field develop, and at t = 56 ms, these increase in amplitude. These low-frequency structures have the characteristics of zonal flows with $k_r > k_{pol}$. The poloidally-symmetric flows do not themselves carry particle flux, but do modulate the measured fluctuation-induced particle flux $\Gamma_{\rm fl}$. It is noteworthy that zonal flows can be produced even in a heliac configuration with very

high helical ripple and without quasi-symmetric properties.

7. Conclusions

Recent research on small and medium stellarators has taken advantage of the diversity in magnetic configurations and operational capabilities to explore basic issues in toroidal confinement. The principal findings are:

- Rational magnetic surfaces play a dual role in determining confinement, alternately enhancing outward transport and encouraging the formation of transport barriers.

- The physics of the plasma response to pressure gradients on or near resonances involves both equilibrium and fluctuations even at low plasma pressure.

- Magnetic islands modify locally flows and radial electric fields, and can function as miniature confinement zones and seeds for transitions to enhanced confinement operation.

- The robust MHD stability of currentless stellarators allows the exploration of extreme ranges of configuration parameters, and greatly assists the study of configuration effects on confinement.

- Helical ripple appears to affect global confinement scaling, although the precise physical mechanism ($1/\nu$ transport, direct losses, flow, trapped particle instabilities, etc.) is unclear at present. The prospects for the performance of a new generation of optimised stellarators with reduced ripple are promising.

- Low power stellarator plasmas are ideally suited for fundamental studies of plasma turbulence phenomena, including wavenumber-resolved transport, zonal flows, and confinement transitions.

All of these results have application to the study and optimisation of tokamak confinement, and tokamak experiments are increasingly taking account and advantage of three-dimensional geometric effects.

Acknowledgements
I am most grateful for many contributions from experimental stellarator research teams around the world. I would particularly like to acknowledge individual discussions with H. Yamada (NIFS), E. Ascasibar and C. Hidalgo (CIEMAT), A. Dinklage and C. Beidler (IPP-Greifswald), U. Stroth (University of Kiel), J. N. Talmadge (University of Wisconsin), D. Brower (University of California at Los Angeles), J. F. Lyon and D. A. Spong (Oak Ridge National Laboratory, USA), and B. D. Blackwell D. G. Pretty and M. G. Shats of the Australian National University.

This work was supported by the Australian Research Council, the Australian Department of Education Science and Training Major National Facilities and Innovation Access Programs, and the Australian Institute for Nuclear Science and Engineering.

References

(please note that page numbers will become available for the "in press" references in August, 2004).

Alejaldre C *et al* 2001 *Nucl. Fusion* **42** 1449
Ascasibar E *et al* 2002 *Plasma Phys. Control. Fusion* **44** B307
Beidler . C D and Hitchon W N G 1994 *Plasma Phys. Control. Fusion* **36** 317
Beidler . C D *et al* 2001 *Nucl. Fusion* **41** 1759
Boozer A H 1984 *Phys. Fluids* **27** 2055
Boozer A H 2004 *Rev. Mod. Phys* in press
Brakel R *et al Plasma Phys. Control. Fusion* **39** 1997 B273
Carreras B A *et al* 1988 *Nucl. Fusion* **28** 1613
Deng C *et al* private communication
Erckmann V *et al* 1993 *Phys. Rev. Lett.* **70** 2086
Estrada T *et al* 2004 *Plasma Phys. Control. Fusion* **46** 277
Evans T E *et al* 2004 *Phys. Rev. Lett.* **92** 235003-1
Feist J-H *et al* 200*4 Fusion Science Technol.* **46** 192
Furth H P *et al* 1963 *Phys. Fluids* **6** 459
Fujisawa A. 200*4 Fusion Science Technol.* **46** 91
Geiger J *et al* 200*4 Fusion Science Technol.* **46** 13
Gerhardt S *et al* 2004 *Phys. Rev. Lett.* submitted
Hamberger S M *et al* 1990 *Fusion Technol.* **17** 123
Harris J H *et al* 1985 *Nucl. Fusion* **25** 623
Harris J H *et al* 1989 Phys. Rev. Lett. **63**, 1249
Harris J H *et al* 2004 *Nucl. Fusion* **44 279**
Herranz J 2000 *Phys. Rev. Lett.* **85** 4715
Hidalgo C *et al* 2002 *New Journal of Physics* 4, 51.1-51.12
Ichiguchi K *et al* 200*4 Fusion Science Technol.* **46** 34
Ida K et al 2004 *Nucl. Fusion* **44** 290
Jayakumar R *et al* 2004 *Fusion Science Technol.* in press
Joffrin E *et al* 2002 *Plasma Phys. Control. Fusion* **44** 1739
Kleiber R *et al 2003 Nucl. Fusion* **44** 686
Lechte C *et al* 2004 *Phys. Rev. Lett* submitted
Likin K M *et al* 2003 *Plasma Phys. Control. Fusion* **45** A133
Lopes Cardozo N J *et al* 1997 *Plasma Phys. Control. Fusion* **39** B303
McCormick K *et al* 2002 *Phys. Rev. Lett.* **89**, 015001
Melnikov A *et al*, 2004, *Fusion Science Technol.* in press
Motojima O. *et al* 2003 *Nucl. Fusion* **43** 1674
Motojima O. *et al* 2004 *Fusion Science Technol.* **46** 1
Murakami S *et al Nucl. Fusion* **39** 1165
Murakami S *et al* 2004 *Fusion Science Technol.* in press
Nemov V V *et al* 2003 *Plasma Phys. Control. Fusion* **45** 43
Ochando M A 2003 *Plasma Phys. Control. Fusion* **45** 221
Okada H *et al* 1995 *Nucl. Fusion* **36** 465
Okamura S *et al* 1995 *Nucl. Fusion* **35** 283
Okamura S *et al* 1999 *Nucl. Fusion* **39** 1337
Okamura S *et al* 2001 *Nucl. Fusion* **41** 1865
Otte M *et al* 2003 *Europhysics Conf. Abs.* **27A**, P-1.9
Pedrosa M A *et al* 2004 *Plasma Phys. Control. Fusion* **46**, 22
Reiman A *et al* 1999 *Plasma Phys. Control. Fusion* **41** B273

Sakakibara S *et al* 2002 *Plasma Phys. Control. Fusion* **44** A217
Sakakibara S *et al* 2004, *Europhysics Conf. Abs.* **30A**, 04-01
Sano F *et al* 2004 *Fusion Science Technol.* in press
Shaing K 2002 Phys. Plasmas **9**, 3470
Scott, B Plasma Phys. Controll. Fusion 39, 1635 (1997)
Shats M G *et al* 1996 *Phys. Rev. Lett.* **77** 4190
Shats M G and Solomon W. M. 2002 *Phys. Rev. Lett.* **88** 045001
Shats M G *et al* 2004 *Fusion Science Technol.* in press
Spong D A *et al* 2004 *Fusion Science Technol.* **46** 215
Stroth U *et al* 1996 *Nucl. Fusion* **36** 1063-1077
Terry P W *Rev. Mod. Phys.* **72** 2000 109 Tribaldos, V 2001 *Phys. Plasmas* **8** 1229
Watanabe K Y *et al* 2004 *Fusion Science Technol.* **46** 24
Yamada H *et al* 2004 *Fusion Science Technol.* **46** 82 Yamada H *et al* 2004 *Europhysics Conf. Abs.* **30A**, P5-099

Figures

1. Variation of stored plasma energy as a function of edge rotational transform in W7-AS. Measurements are shown by the data points; model results are shown by the line.

2. Fluctuation experiment on the HSX stellarator. (a) Mod-B maps for the quasi-helically symmetric (QHS) configuration, and the "mirror" configuration in which the quasi-symmetry is spoiled by a 10% additional toroidal field component. (b) Density fluctuation during a 50 kW ECH discharge in the QHS configuration. (c) Comparison of X-ray spectra in the QHS and mirror configurations.

3. External magnetic fluctuations in 60 kW ICRF discharges in the H-1NF heliac with rotational transform profiles crossing (a) the ι = 5/4 and 9/7 resonances, and (b) the ι = 6/5 and 5/4 resonances.

4. (a) Magnetic surfaces for TJ-II heliac configurations without (left) and with (right) edge magnetic islands at ι = 2. (b) Mach probe measurements of plasma flow in configurations with and without islands. ECH power 300 kW. (c) Heavy-ion beam probe measurements of potential profiles in configurations with and without islands. ECH power 600 kW.

5. Normalised scaling of energy confinement time in stellarators compared to provision ISS04 scaling relation. The normalisation factors f_{enh} depend on configuration.

6. Flux surfaces for nominal and shifted in CHS configurations (similar to LHD) and computed trapped particle orbits for reactor scale configuration (in Boozer flux coordinates).

7. Variation of configuration dependent factor f_{enh} with effective helical ripple.

8. Plasma flow speeds induced in HSX plasmas (50 kW ECH) by electrode biasing in quasi-helically symmetric (QHS) and mirror configurations.

9. Turbulence studies in low temperature plasmas in the TJ-K experiment. (a) Comparison of cross-phase between density and potential fluctuations for three working gases and numerical calculations using the DALF code. (b) scaling of poloidal correlation length of teh turbulence.

10. Development of zonal flows in an H-mode discharge in the H-1NF heliac.

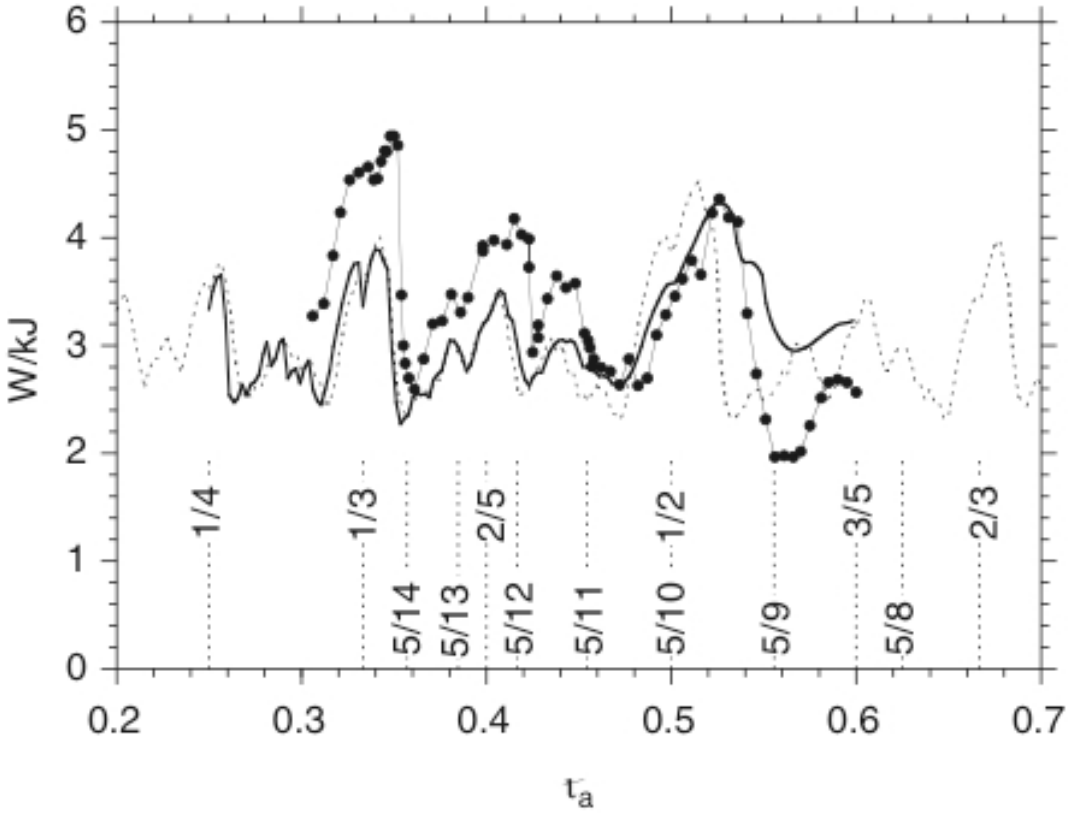

Harris, Fig. 1

$$\text{QHS}: \quad B/B_o \approx 1+\varepsilon_H \cos(4\varphi-\theta)$$

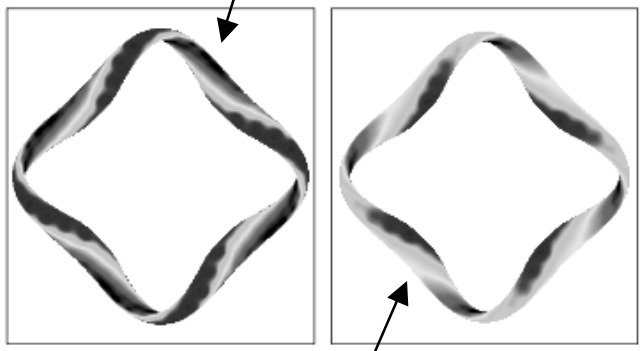

$$\text{Mirror}: \quad B/B_o \approx 1+\varepsilon_H \cos(4\varphi-\theta)+\varepsilon_M \cos(4\varphi)$$

(a)

(b)

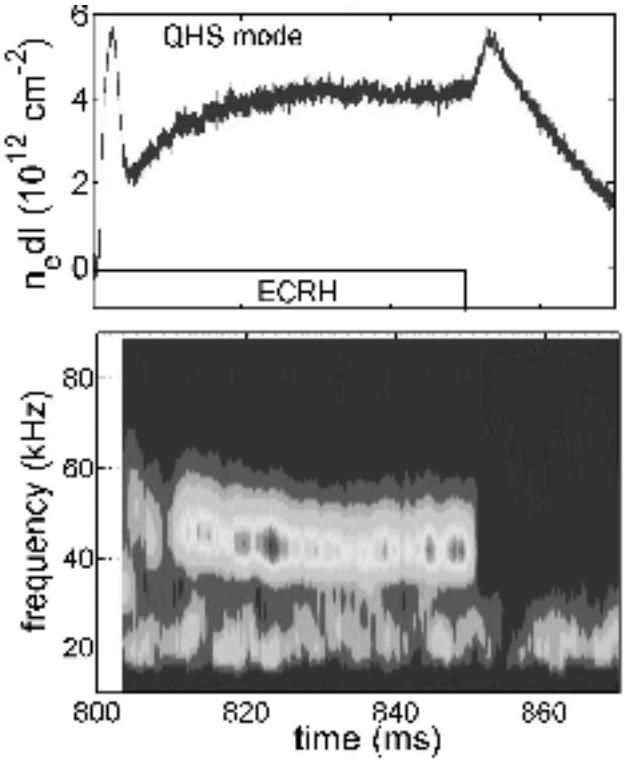

(c)

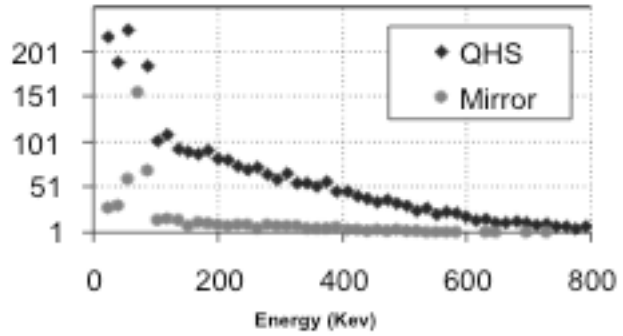

Harris, Fig. 2

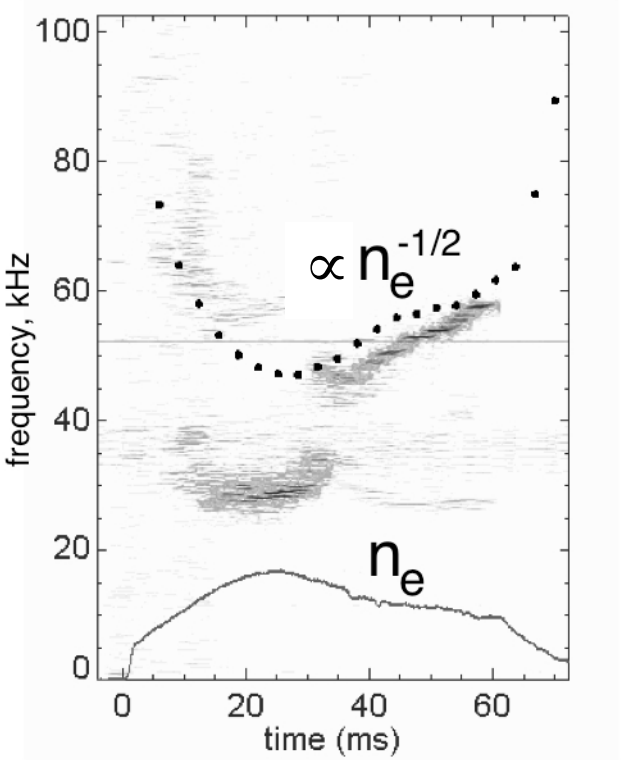

(a)

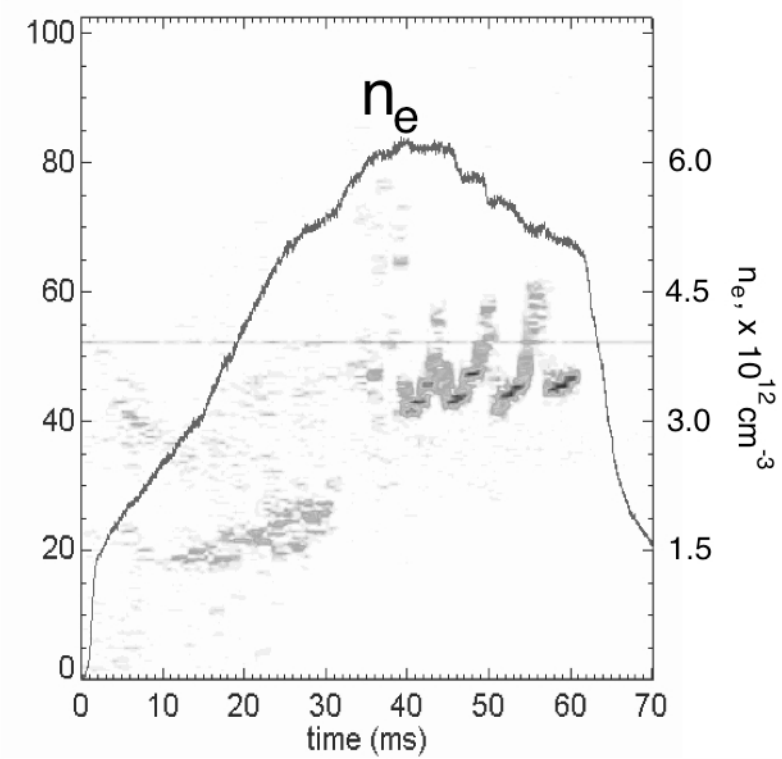

(b)

Harris, Fig. 3

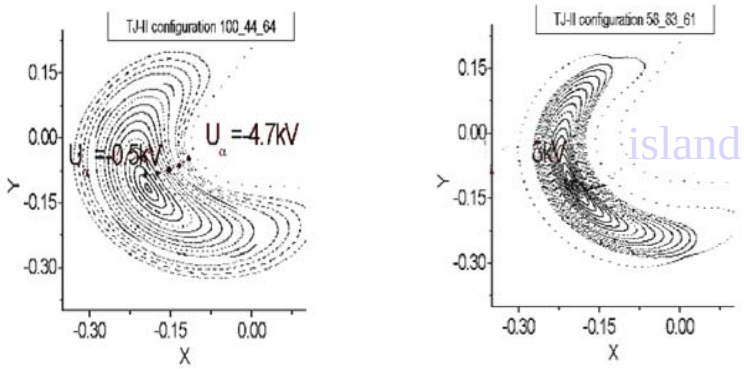

(a)

(b)

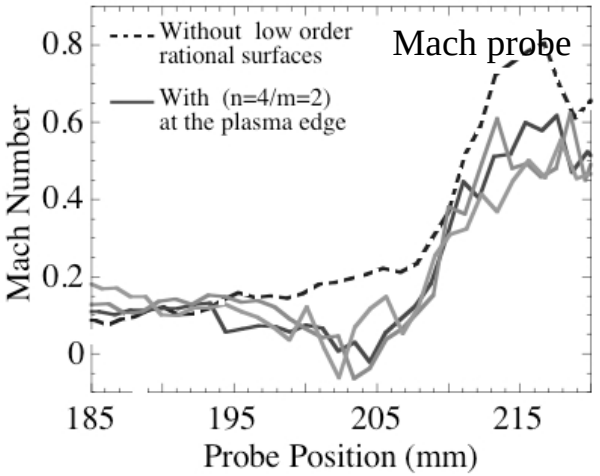

(c)

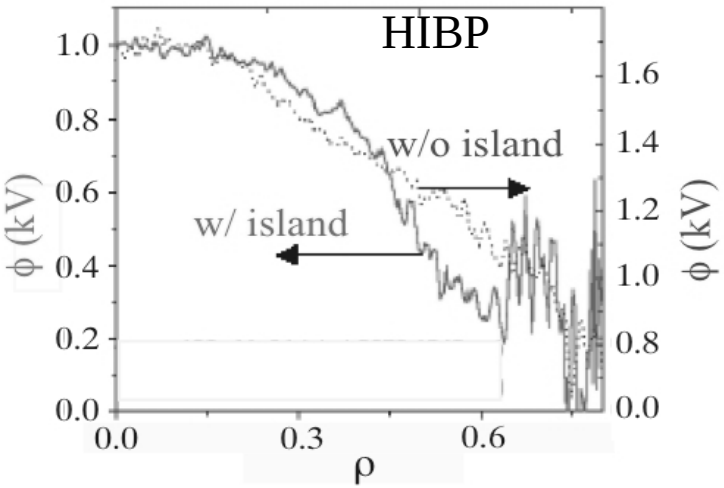

Harris, Fig. 4

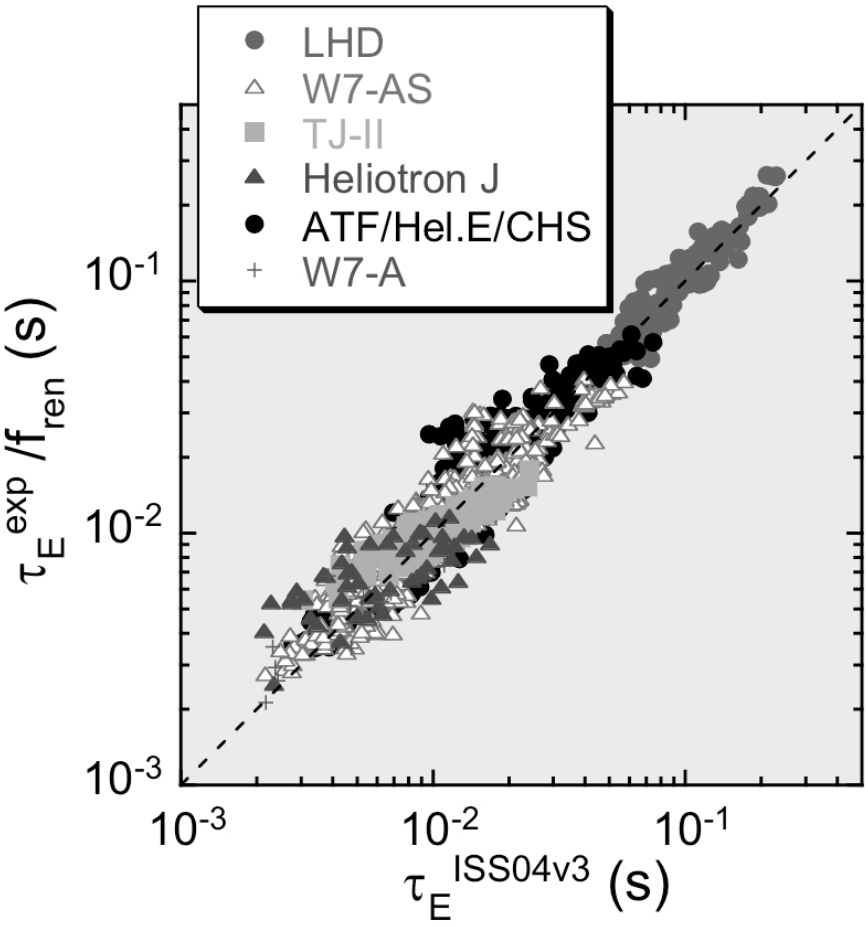
LHD
W7-AS
TJ-II
Heliotron J
ATF/Hel.E/CHS
W7-A
10^{-1}
10^{-2}
10^{-3}
τ_E^{exp}/f_{ren} (s)
10^{-3}
10^{-2}
10^{-1}
$\tau_E^{ISS04v3}$ (s)

Harris, Fig. 5

nominal shifted-in

CHS
(~LHD)
flux surfaces

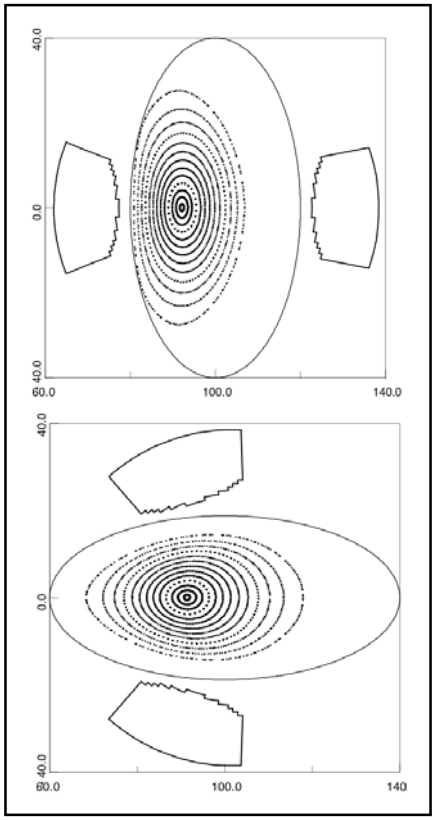

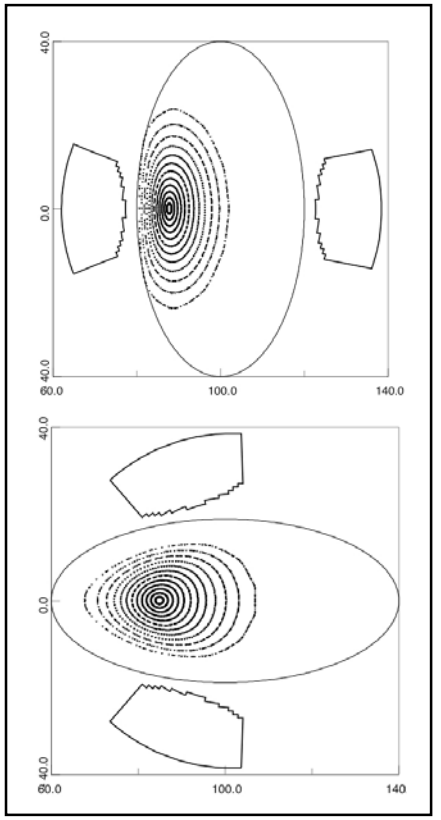

helically
trapped
alpha orbits
(flux coord)
reactor-size
model

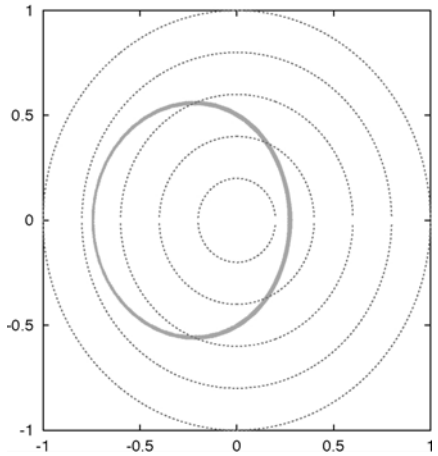

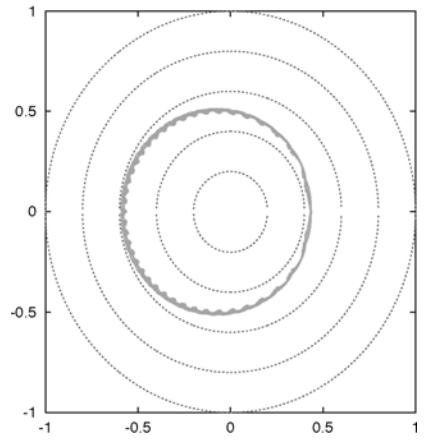

Harris, Fig. 6

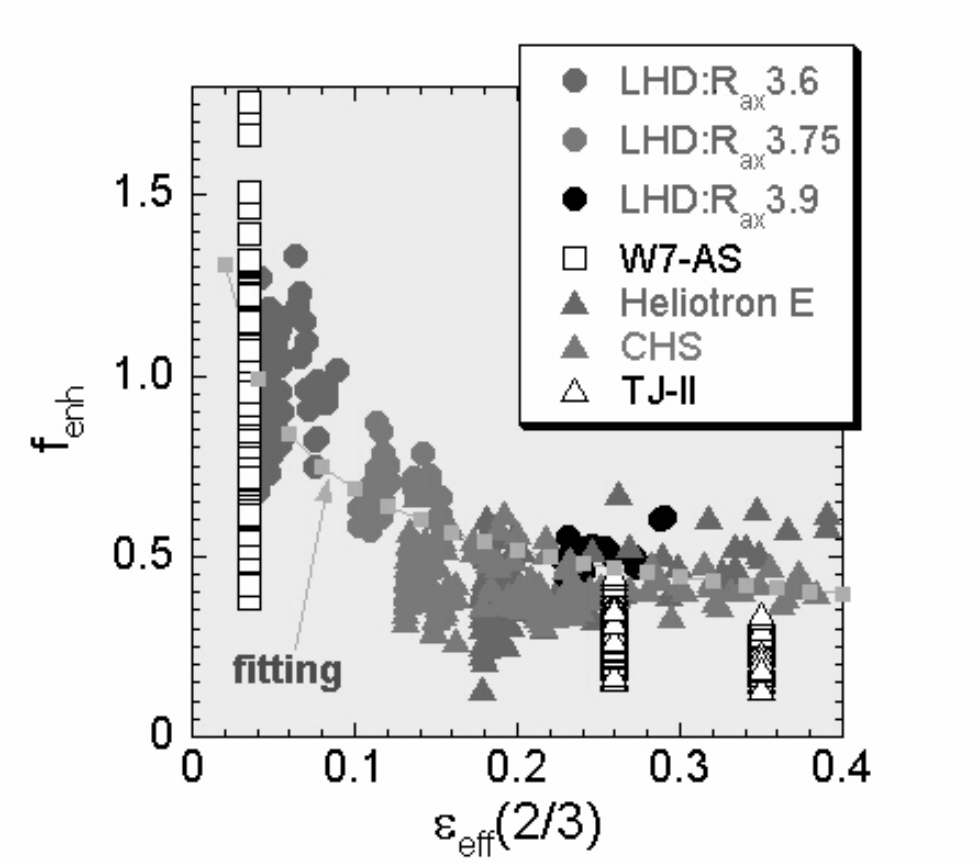
LHD:R$_{ax}$3.6
LHD:R$_{ax}$3.75
LHD:R$_{ax}$3.9
W7-AS
Heliotron E
CHS
TJ-II
fitting
f_{enh}
$\varepsilon_{eff}(2/3)$
0
0.5
1.0
1.5
0.1
0.2
0.3
0.4

Harris, Fig. 7

Flow speed (Mach)

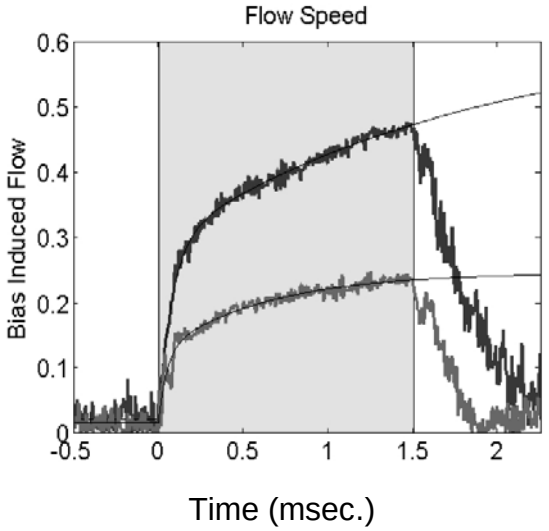

QHS: 8 A of electrode current

Mirror: 10 A of electrode current

Harris, Fig. 8

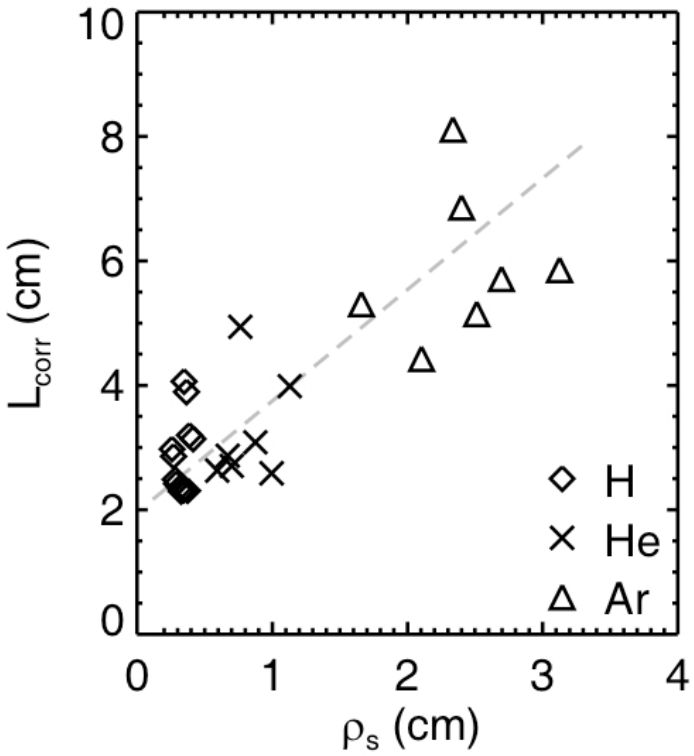

Harris, Fig. 9

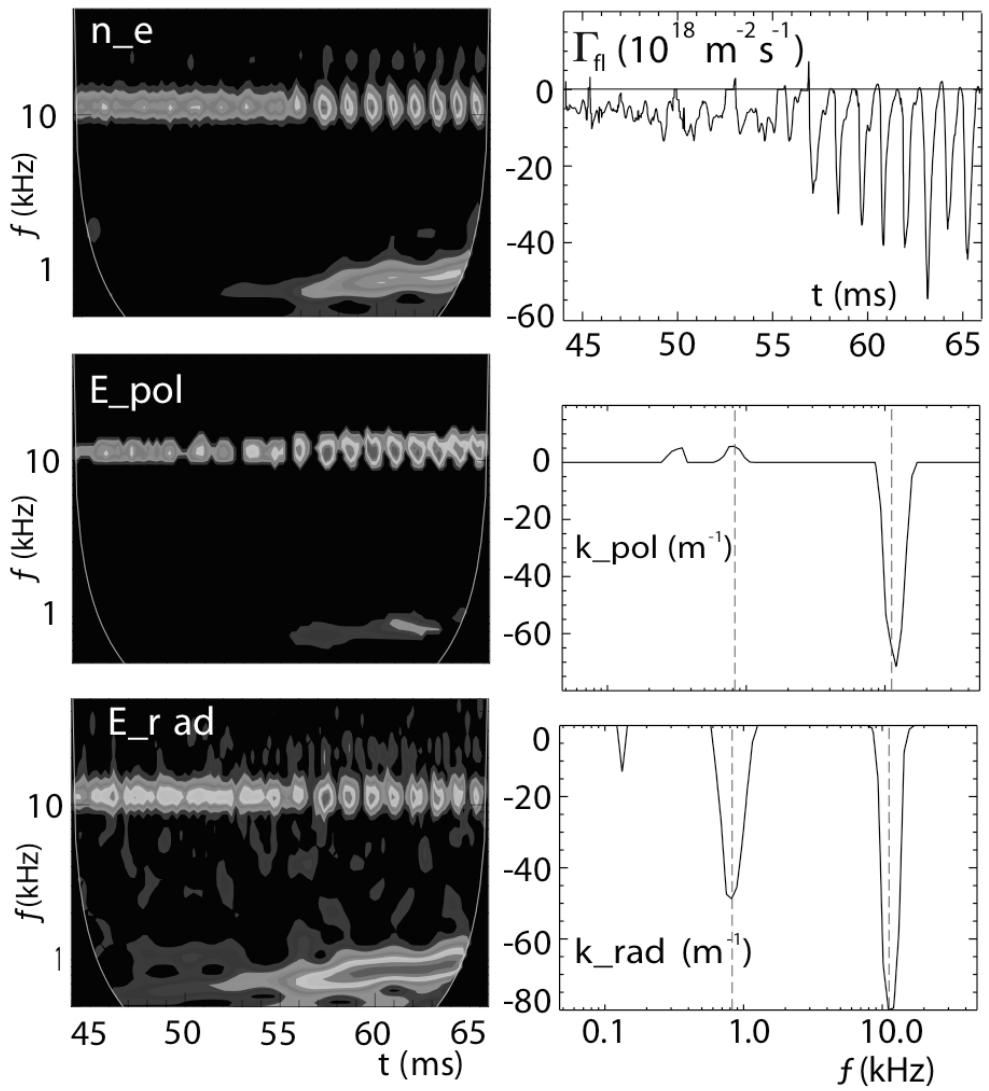

Harris, Fig. 10